Magnetic structure of Ce_2RhIn_8: Evidence for ordered moments on the Rh sites

A. Schenck and F. N. Gygax
Institute for Particle Physics of ETH Zürich (IPP), 5232 Villigen PSI, Switzerland

T. Ueda and Y. Ōnuki
Graduate School of Science, Osaka University, Toyonaka, Osaka 560, Japan
(Received 23 December 2003; published 20 August 2004)

The magnetic properties of heavy fermion Ce_2RhIn_8 have been studied by zero-field (ZF) and transverse-field muon spin rotation spectroscopy (μSR). In ZF below $T_N=28$ K 2/3 of the implanted μ^+ experience a spontaneous field $\boldsymbol{B}_\mu$ which is confined to the surface of a cone oriented along the c axis with an aperture of $\sim 40°$ and, at 1.8 K, amounts to 44 G. The remaining μ^+ fraction experiences a zero average field. The appearance of a field component parallel to the c axis is incompatible with the magnetic structure determined by neutron scattering [W. Bao *et al.*, Phys. Rev. B **64**, 020401(R) (2001)] and in line with μSR measurements on $CeRhIn_5$ [A. Schenck *et al.*, Phys. Rev. B **66**, 144404 (2002)]. To remove the incompatibility it is proposed that, as in $CeRhIn_5$, the Rh sublattice also carries ordered moments. Possibilities for their arrangement are discussed. Additional μ^+ Knight shift measurements yielded very similar results as in $CeRhIn_5$ and imply that the μ^+ occupy corresponding sites in Ce_2RhIn_8.

DOI: 10.1103/PhysRevB.70.054415 PACS number(s): 75.25.+z, 76.60.Cq, 76.60.Jx, 76.75.+i

I. INTRODUCTION

A recent muon spin rotation spectroscopy (μSR) study of the tetragonal heavy fermion compound $CeRhIn_5$[1] yielded the unexpected result that the observed four different spontaneous internal fields in the antiferromagnetic phase could not be reproduced on the basis of the helical incommensurate antiferromagnetic structure determined by neutron scattering[2] and nuclear quadrupole resonance (NQR).[3] According to Refs. 2 and 3 the ordered moments are confined to the (a,b) plane and the spiral axis is oriented along the c axis with a propagation vector of $\boldsymbol{q}=(\frac{1}{2}\frac{1}{2}\delta)$ and $\delta=0.297$. This leads to dipolar fields with a unique value of ~ 60 G at the interstitial a site $(\frac{1}{2}\frac{1}{2}\frac{1}{2})$, which is occupied by about 66% of the implanted μ^+.[1] This field is strictly confined to the (a,b) plane but rotates by an angle of 107° from plane to plane. The simple antiferromagnetic arrangement of the moments within the basal plane results in zero contact hyperfine fields at the a sites. However, the experiment yielded internal fields $\boldsymbol{B}_\mu$ which were confined to the surface of cones with different apertures, implying sizable components along the c axis, $\boldsymbol{B}_\mu^{\parallel}$. Also the perpendicular in-plane component $\boldsymbol{B}_\mu^{\perp}$ was smaller than expected. It was also found from μ^+ Knight shift measurements that the field-induced moments on the Ce sites were insufficient to explain the resulting dipolar fields at the μ^+. All this led to the conclusion that the discrepancies between the measurements and the expectations may be attributed to the Rh ions which must possess magnetic moments of their own. The Knight shift results indicate that the moments $\boldsymbol{\mu}_{\mathrm{Rh}}$ on the Rh site could be induced by the neighboring Ce ions and, if so, would be given by $\boldsymbol{\mu}_{\mathrm{Rh}}=-0.08\boldsymbol{\mu}_{\mathrm{Ce}}$.[1] This then explained the reduced field in the basal plane in the ordered state. The appearance of different c axis components of $\boldsymbol{B}_\mu$, however, had to be explained by postulating that the c axis component of the moments on the four nearest Rh neighbors around the μ site can be aligned parallel or pairwise antiparallel or something in between. It was conjectured that the Ce moments along the c axis are coupled via the intervening Rh ions by super exchange and that competing exchange and super exchange couplings could explain the helical structure. The magnitude of the magnetic moments on the Rh sites was estimated to be below 0.1 μ_B, too small to be noticed in the neutron and NQR experiments. In fact, in Ref. 2 the presence of magnetic moments on the Rh sites was explicitly ruled out. Of course the question arouse immediately whether the behavior of the Rh sublattice is unique to $CeRhIn_5$ or can also be observed in other compounds. In pursuit of this question we have started a program to investigate other Rh containing intermetallic compounds. In this contribution we report on μSR measurements of Ce_2RhIn_8 which possesses a structure which is rather similar to $CeRhIn_5$. It contains the $CeRhIn_5$ unit cell as building blocks separated by planes containing just In atoms (see Fig. 1). Alternatively one can view Ce_2RhIn_8 to consist of a stack of $CeIn_3$ unit cells along the c axis separated by layers of In and Rh. $CeRhIn_5$ and Ce_2RhIn_8 as well as $CeIn_3$ belong to the $Ce_nM_mIn_{3n+2m}$ family of structures. $CeRhIn_5$ and Ce_2RhIn_8 also belong to the class of so-called heavy fermion systems, the latter compound possessing a Sommerfeld constant of $\gamma\simeq 0.4$ J/mol CeK^2 (Ref. 4). Ce_2RhIn_8 crystallizes in the tetragonal Ho_2CoGa_8 structure (space group No. 123) with lattice parameters $a=4.665$ Å and $c=12.244$ Å at room temperature. The corresponding lattice constants in $CeRhIn_5$ are $a=4.65$ Å and $c=7.54$ Å. Hence the distance of Ce ions across the Rh site is about 10% larger in Ce_2RhIn_8 than in $CeRhIn_5$ while the distance in the basal plane is only marginally larger. However, the distance between Ce ions across the In plane at $z=\frac{1}{2}$ in Ce_2RhIn_8 amounts to only ~ 4.5 Å, similar to the case in $CeIn_3$, and so one may expect that those Ce ions are strongly magnetically interacting.

The magnetic structure of Ce_2RhIn_8 has been investigated by neutron scattering.[5] A simple antiferromagentic structure,

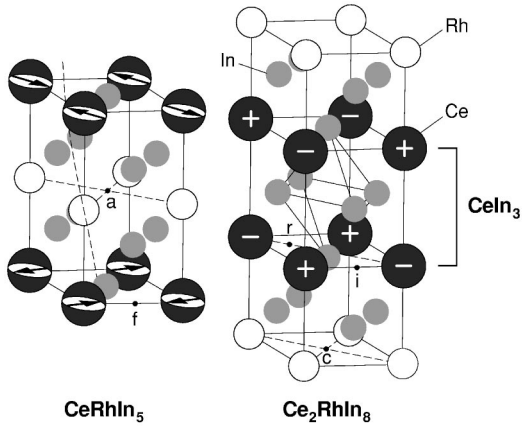

FIG. 1. Comparison of the crystal and magnetic structures of $CeRhIn_5$ and Ce_2RhIn_8. The center part of the latter corresponds to $CeIn_3$, the lower and upper parts each to one half of the unit cell of $CeRhIn_5$ (adapted from Ref. 5). The *a* and *f* sites in $CeRhIn_5$ and the *c*, *r*, and *i* interstitial sites in Ce_2RhIn_8 are indicated.

as depicted in Fig. 1, has been found with an ordered moment of $\sim 0.55\ \mu_B$ at 1.6 K tilted away from the *c* axis by $\sim 38°$. The direction of the in-plane component has not been determined. As we will see below, the μSR results allow one to suggest a likely scenario for the arrangement of the in-plane components.

II. EXPERIMENTAL DETAILS

In the present experiment we used a single crystal grown by the In-flux method at Osaka University[6] which had a plate-like shape with dimensions of roughly $3 \times 2.5 \times 1\ mm^3$. The *c* axis was perpendicular to the large plane and the *a* axis parallel to the short edge of that plane. The μSR experiments were performed at the Paul Scherrer Institut using the general purpose spectrometer on the πM3 beamline, providing 100% spin polarized μ^+ with a momentum of 28 MeV/*c*. The sample was mounted in a He-flow cryostat allowing us to set temperatures between 1.8 and 300 K. The sample could be rotated inside the cryostat around the *a* axis which was oriented perpendicular to the beam momentum in the horizontal plane. The external field for the transverse-field (TF) measurements was applied along the beam momentum. A spin rotator in the μ^+ beamline allowed us to turn the μ^+ spin polarization by $\sim 45°$ from the horizontal towards the vertical direction, which condition was used for the TF as well as the zero-field (ZF) measurements. The positrons from the μ^+ decay could be recorded in up, down, forward, backward and right direction with respect to the beam momentum. Although the sample is relatively small, a background-μSR signal from μ^+ stopping outside of the sample was practically not detectable in the TF measurements.

III. TRANSVERSE FIELD (TF) MEASUREMENTS

We begin with the TF measurements ($H_{ext}=6$ kOe) and the determination of the μ^+ sites.[7] As in $CeRhIn_5$ we found

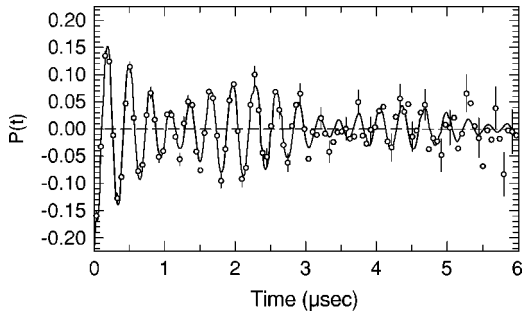

FIG. 2. TF signal at 1.8 K for $\boldsymbol{H}_{ext} \| c$ axis ($H_{ext}=6$ kOe) displayed in a frame rotating at 78 MHz to render the two-component beating visible.

two components in the precession signal (labeled 1 and 2) with significantly different frequency shifts and a temperature independent amplitude ratio of roughly 2:1. The μ^+ spin rotation signal at 5 K and for $\boldsymbol{H}_{ext} \| c$ axis is shown in Fig. 2 in a rotating frame revolving at 78 MHz. The presence of a beating behavior is clearly seen. Figure 3 displays the angular dependence of the Larmor precession frequencies ν_1, ν_2 when $\boldsymbol{H}_{ext}$ is turned in the (b,c) plane. Both frequency shifts follow a $\cos^2\theta$ dependence, the stronger component, 1, showing a much smaller anisotropy than the weaker one, 2. This behavior is essentially the same as in $CeRhIn_5$. From the frequency shifts the Knight shifts K_1 and K_2 are extracted in the usual way by correcting for the demagnetization and Lorentz field contributions.[7] In Fig. 4 K_1 and K_2 are plotted versus the bulk susceptibility χ (Clogston–Jaccarino plot), the latter taken from Ref. 5. We find that K_1 and K_2 scale with χ below 110 K down to 40 K if $\boldsymbol{H}_{ext} \| c$ axis, and down to 5 K (7.5 K) (the lowest temperature applied) if $\boldsymbol{H}_{ext} \perp c$ axis. The loss of scaling above 110 K (data are not shown) is probably arising from the onset of long range μ^+ diffusion for $T \geqslant 140$ K. Interestingly, at low *T* the scaling is lost only for $\boldsymbol{H}_{ext} \| c$ axis. The slopes $A_i^{\|,\perp} = dK_i^{\|,\perp}/d\chi_{\|,\perp}$ ($\|$ indicates $\boldsymbol{H}_{ext} \| c$ axis and $\perp$ $\boldsymbol{H}_{ext} \perp c$ axis) in the scaling regime are listed in Table I together with the corresponding results from $CeRhIn_5$.[1] As can be seen, they are qualitatively similar and indicate that the μ^+ are localized at corresponding sites.

The slopes $A_i^{\|,\perp}$ consist of a dipolar field contribution $A_{\varrho\varrho,i}^{dip}$ ($\varrho\varrho = aa, bb, cc$) and a contact hyperfine field contribu-

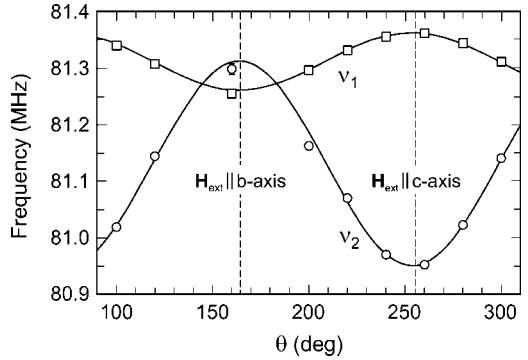

FIG. 3. Orientation dependence of the Larmor precession frequencies ν_1 and ν_2 at 20 K [the applied field H_{ext} is rotating in the (b,c) plane]. The solid lines represent $\cos^2\theta$ fits.

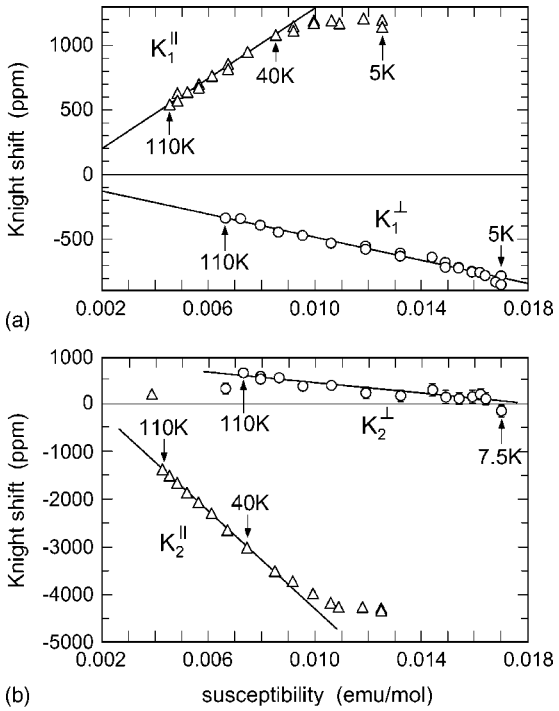

FIG. 4. Clogston–Jaccarino plots of (a) K_1 and (b) K_2 for $\boldsymbol{H}_{\rm ext}\|c$ axis and $\boldsymbol{H}_{\rm ext}\perp c$ axis. The susceptibility data are taken from Ref. 5.

tion $A_{0,i}$, e.g., $A_i^{\parallel}=A_{cc,i}^{\rm dip}+A_{0,i}$, where $A_{cc,i}^{\rm dip}$ is a diagonal element of the dipolar coupling tensor $\overleftrightarrow{A}_{\rm dip}$.[7] The fact that the two observed components show no further splitting when $\boldsymbol{H}_{\rm ext}$ is rotated with respect to the crystal frame, and that the $\nu_i(\theta)$ assume an extremum at $\boldsymbol{H}_{\rm ext}\|c$ axis or $\boldsymbol{H}_{\rm ext}\perp c$ axis, as evidenced in Fig. 3(a), implies that $\overleftrightarrow{A}_{\rm dip}$ contains only diagonal elements and that $A_{aa}^{\rm dip}=A_{bb}^{\rm dip}=-\frac{1}{2}A_{cc}^{\rm dip}$,[7] where a,b,c refer to the corresponding crystal axes. Assuming further that the contact coupling constant A_0 is temperature independent and isotropic, we derive from $A_i^{\parallel,\perp}$ the parameters $A_{0,i}$ and $A_{cc,i}^{\rm dip}$ listed also in Table. I. $\overleftrightarrow{A}_{\rm dip}$ depends on the μ^+ site and the host crystal structure and can be easily calculated. The observed axially symmetric form of $\overleftrightarrow{A}_{\rm dip}$ is only reproduced for the axially symmetric interstitial sites $1b,1c$ and $1d$ (in Wyckoff notation). Calculated values for $A_{cc}^{\rm dip}$ are listed in Table II. Comparing these values with the experimental $A_{cc,i}^{\rm dip}$ in Table I, we find no obvious agreement.

Concerning component 1, closest agreement is found if the μ^+ is placed at the c site, corresponding to the a site in $CeRhIn_5$. On the other hand, the large negative value of $A_{cc,2}^{\rm dip}$ seems to be incompatible with any of the axially symmetric sites. The same situation was encountered in $CeRhIn_5$.[1] Following Ref. 1 we conclude that the majority signal 1 can only arise from μ^+ located at the c-site and that the measured and calculated $A_{cc,1}^{\rm dip}$ can be reconciled by postulating that the Rh sublattice also contributes to the μ^+ Knight shifts. Hence we write

$$K_1^{\parallel,\perp}=K_1^{\parallel,\perp}({\rm Ce})+{\rm K}_1^{\parallel,\perp}({\rm Rh}) \tag{1}$$

and

TABLE I. Compilation of measured $A_i=dK_i/d\chi_i(i=1,2)$ and derived $A_{cc,i}^{\rm dip}$ and $A_{0,i}$ in $CeRhIn_5$ and Ce_2RhIn_8 for $\boldsymbol{H}_{\rm ext}\|c$ axis and $\boldsymbol{H}_{\rm ext}\perp c$ axis (in kG/μ_B).

	$A_1^{\parallel}$	$A_1^{\perp}$	$A_2^{\parallel}$	$A_2^{\perp}$
$CeRhIn_5$	0.257 (6)	−0.424(17)	−1.41(3)	1.1 (4)
Ce_2RhIn_8	0.743 (13)	−0.249(7)	−2.87(2)	−0.267(30)
	$A_{cc,1}^{\rm dip}$	$A_{0,1}$	$A_{cc,2}^{\rm dip}$	$A_{0,2}$
$CeRhIn_5$	+0.45(2)	−0.19(3)	−1.67(27)	0.26 (30)
Ce_2RhIn_8	+0.66(2)	+0.083(9)	−1.74(5)	−1.14(3)

$$\chi_{\rm bulk}^{\parallel,\perp}=\chi_{\rm Ce}^{\parallel,\perp}+\chi_{\rm Rh}^{\parallel,\perp}. \tag{2}$$

The scaling behavior, displayed in Fig. 4, implies that

$$\chi_{bulk}^{\parallel,\perp}=(1+\alpha)\chi^{\parallel,\perp}({\rm Ce}) \tag{3}$$

with α a temperature independent constant, i.e., the functional form of the temperature dependence of χ(Ce) and χ(Rh) is the same. This could imply that the moments on the Rh sites are induced via the induced moment on the Ce sites by an indirect mechanism. Proceeding as in Ref. 1 [using Eqs. (3), (4), (5) in Ref. 1], we estimate that $\alpha=-0.106$ (in $CeRhIn_5$ $\alpha=-0.08$). Alternatively, considering only moments on the Ce sites, one may trace back the difference between the calculated and measured $A_{cc}^{\rm dip}$ to our assumption of an isotropic and temperature independent A_0. Dropping this assumption and postulating that $A_{cc}^{\rm dip}$ is given by the calculated value, one can estimate $A_0^{\parallel,\perp}$ from

$$A_1^{\parallel,\perp}=A_{cc/aa}^{\rm dip}+A_0^{\parallel,\perp}. \tag{4}$$

While such a scenario seems to be realized in systems showing quadrupolar effects, e.g., in CeAg,[8] we do not think that it applies to $CeRhIn_5$ or Ce_2RhIn_8, in particular because it does not help in explaining the zero-field results in the ordered state.

Concerning the minority signal, 2, it appears impossible to attribute the large negative $A_{cc,2}^{\rm dip}$ to the magnetic response of the Rh sublattice. The large negative value implies that the μ^+ is located somewhere in the CeIn plane. In fact, the extracted $A_{cc,2}^{\rm dip}$ is close to the calculated value for the i sites and in $CeRhIn_5$ it agrees perfectly with the calculated value for the equivalent f site. However, the i sites (or the f sites in $CeRhIn_5$) split into two magnetically inequivalent subsites (see Table II) and consequently the signal 2 should also have shown a splitting for $\boldsymbol{H}_{\rm ext}\perp c$ axis which is not seen. Another in principle possible site is the $8r$ site. The site possesses the interesting property that $A_{aa}=A_{bb}=\frac{1}{2}A_{cc}$ but $A_{i\neq j}\neq 0$. The latter leads to a splitting and phase shifted angular dependencies, but for $\boldsymbol{H}_{\rm ext}\|c$ axis and $\boldsymbol{H}_{\rm ext}\perp c$ axis there will be no splitting. This is again in contradiction with the data shown in Fig. 3. The only possibility, we can propose at present, is to assume that the μ^+ hops very quickly between the $4i$ or the $8r$ sites which would lead to $\langle A_{aa}^{\rm dip}\rangle=\langle A_{bb}^{\rm dip}\rangle=0$ or $\langle A_{i\neq j}\rangle=0$, respectively, leaving $\langle A_{cc}^{\rm dip}\rangle$ unchanged. One may speculate that the μ^+ associated with the signal 2 are in a tunneling

TABLE II. Compilation of calculated A_{ii}^{dip} (in kG/μ_B) for different interstitial sites arising from parallel aligned moments on the Ce or Rh sites. Generally $A_{i\neq j}=0$, except for the 8*r* sites. Lattice constants used: $a=4.665$ Å, $c=12.244$ Å.

Site	Position (s)	Sublattice	A_{aa}^{dip}	A_{bb}^{dip}	A_{cc}^{dip}
1*b*	$(0\ 0\ \frac{1}{2})$	Ce	−1.406	−1.406	+2.812
		Rh	−0.156	−0.156	+0.312
1*c*	$(\frac{1}{2}\ \frac{1}{2}\ 0)$	Ce	−0.230	−0.230	+0.460
		Rh	+0.614	+0.614	−1.228
1*d*	$(\frac{1}{2}\ \frac{1}{2}\ \frac{1}{2})$	Ce	+0.124	+0.124	−0.248
		Rh	−0.147	−0.147	+0.294
4*i*	$(0\ \frac{1}{2}\ 0.315)$	Ce	−1.277	2.834	−1.557
		Rh	−0.18	−0.11	+0.29
	$(\frac{1}{2}\ 0\ 0.315)$	Ce	2.834	−1.277	−1.557
		Rh	−0.18	−0.18	−0.29
8*r*	(*xxz*)	Ce	$A_{aa}=A_{bb}=-\frac{1}{2}A_{zz}$, but $A_{i\neq j}\neq 0$		

state around the In atom in the CeIn plane connecting the four 8*r* sites next to the In atom. As we will see, this also explains that in the ordered state no net spontaneous field is experienced by those μ^+.

In conclusion, we find the μ^+ to occupy equivalent sites in $CeRhIn_5$ and Ce_2RhIn_5, namely, the majority signal in the 1*a* or 1*c* site, respectively, and the minority signal most likely being in a tunneling state around the In atom in the CeIn plane. Further, the Rh ions aquire a magnetic moment through an indirect antiferromagnetic coupling to the Ce ions.

IV. ZERO-FIELD (ZF) MEASUREMENTS

Next we turn to the ZF measurements below T_N. Some typical signals are displayed in Fig. 5. Below T_N the time evolution of the μ^+ polarization is best fitted by the expression

$$P(t) = A_\omega e^{-\frac{1}{2}\sigma_1^2 t^2} \cos\ \omega t + A_\lambda e^{-\frac{1}{2}\sigma_2^2 t^2}, \tag{5}$$

which changes to a single component exponential decay just above $T_N \simeq 2.8$ K. In contrast to $CeRhIn_5$, below T_N only a single oscillating component is present revealing a spontaneous internal field of $B_\mu \sim 44$ G at 1.8 K. The amplitude A_1 shows a pronounced dependence on the orientation of the crystal as it is turned around the *a* axis with the initial polarization $\boldsymbol{P}(0)$ lying in the (b,c) plane (see Fig. 6). These data were analyzed in the same fashion as in $CeRhIn_5$ by considering different directions for the internal field $\boldsymbol{B}_\mu$.[1] We found that the only arrangement consistent with the tetragonal symmetry of the sample consisted, as in $CeRhIn_5$, of a conical arrangement of $\boldsymbol{B}_\mu$ with the axis of the cone aligned along the *c* axis and an aperture of $\Omega = 40 \pm 1°$, i.e., Eqs. 12(a) and 12(b) from Ref. 1 were used to fit $A_1(\theta)$ (solid line in Fig. 6). In other words, $\boldsymbol{B}_\mu$ possesses a distinct component along the *c* axis, $B_\mu^{\parallel}$, and a perpendicular component, $\boldsymbol{B}_\mu^{\perp}$, which can assume all possible directions in the (a,b) plane. At 1.8 K $B_\mu^{\parallel} = B_\mu \cos\Omega = 33.7$ G and $B_\mu^{\perp} = B_\mu \sin\Omega = 28.3$ G. This anlysis also revealed that the ratio of the μ^+ fractions contributing to the first and second term in Eq. (5) amounted to ~ 2. Hence the first, oscillating component was identified to arise from the μ^+ stopped at *c* sites and the second component with zero average field from the μ^+ associated with the possible tunneling state. Neither σ_1 nor σ_2 were dependent on the sample orientation.

The temperature dependence of $\nu = \omega/2\pi$ is displayed in Fig. 7; σ_1 decreased from 2.3 μs^{-1} at 1.8 K to ~ 1.8 μs^{-1} at 2.7 K, and $\sigma_2 \simeq 0.5$ μs^{-1} showed essentially no temperature dependence. The equation $\sigma_1 = 2.3$ μs^{-1} translates into a field spread of $\Delta B_\mu \simeq 27$ G, hence $\Delta B_\mu / B_\mu \simeq 0.61$, i.e., the μ^+ contributing to the oscillating signal experience a rather wide field distribution. The temperature dependence of ν is well reproduced by the empirical expression

$$\nu = \nu_0 \left(1 - \left(\frac{T}{T_c}\right)^{\delta}\right)^{\beta} \tag{6}$$

with $T_c = 2.74(1)$ K, $\nu_0 = 0.86(1)$ MHz, $\delta \equiv 1.5$, $\beta \equiv 0.5$ (solid line in Fig. 7). Figure 7 also shows the temperature dependence of the square root of the magnetic Bragg peak intensities from Ref. 5 which is proportional to the magnitude of the ordered moment μ_{Ce}. The temperature dependence is quite different and when fitted by Eq. (6) with $T_N \equiv 2.74$ K and $\delta \equiv 1.5$, yields $\beta = 0.17(1)$. Since one expects that $\nu(T) \propto \mu_{\mathrm{Ce}}(T)$ the difference is puzzling and not understood at present; $\delta = 1.5$ is expected for a ferromagnet and reflects the Bloch $T^{3/2}$ law, $\beta = 0.5$ is expected in the mean field approximation.

How consistent are the μSR results with the antiferromagnetic structure determined by neutron scattering? Using the information from Ref. 5 we have calculated the dipolar fields $\boldsymbol{B}_{\mathrm{dip}}$ at the 1*c* site and the 4*i* and 8*r* sites at 1.8 K, following the recipe of Pinkpank and Andreica.[7] Since the direction of the component of the ordered moments $\boldsymbol{\mu}_{Ce}$ in the (a,b) plane was not determined, we had to make some assumption about their behavior. In view of that the $CeIn_3$-building block in Ce_2RhIn_8 has essentially the same dimensions as $CeIn_3$ we

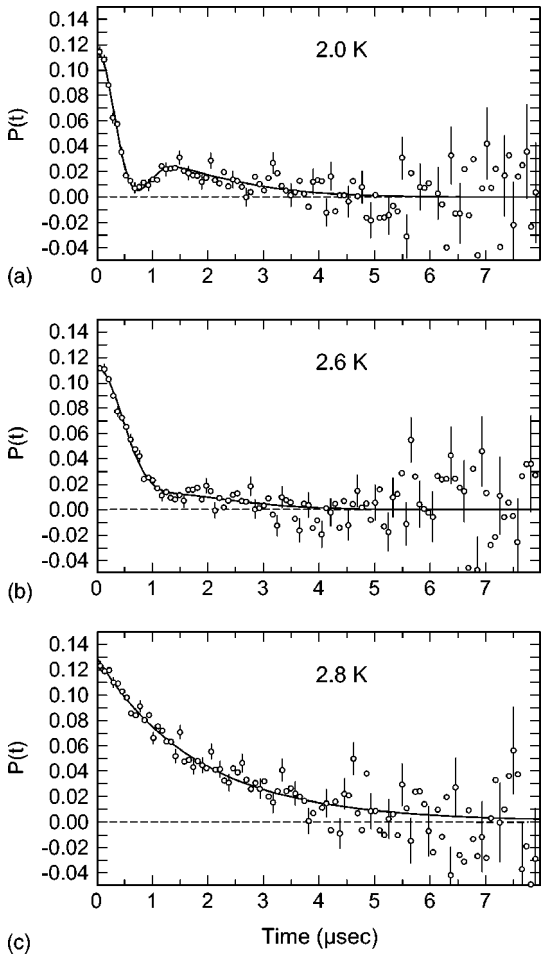

FIG. 5. ZF-μSR signal $P(t)$ at (a) 2 K, (b) 2.6 K and (c) 2.8 K. The solid lines in (a) and (b) are fits of Eq. (5) to the data. The solid line in (c) represents a simple exponential decay.

assume that the in-plane components $\boldsymbol{\mu}_{Ce}^{\perp}$ inside a $CeIn_3$ unit are, like in $CeIn_3$, strictly antiferromagnetically correlated, but that from building block to building block the phase of the in-plane component $\boldsymbol{\mu}_{Ce}^{\perp}$ changes either randomly or progressively with a certain propagation vector $\boldsymbol{q}$, like in $CeRhIn_5$.

We first consider now the 1*c* site. As the calculations show, a random orientation of $\boldsymbol{B}_{\mu}^{\perp}$ is only possible if the in-plane component $\boldsymbol{\mu}_{Ce}^{\perp}$ assumes likewise all possible orientations.

Specifically the calculations produce $B_{\mathrm{dip}}^{\parallel}=0$ along the *c* axis at the 1*c* site owing to the antiferromagnetic arrangement of the $\boldsymbol{\mu}_{\mathrm{Ce}}^{\parallel}$ and independent of the assumptions made on $\boldsymbol{\mu}_{Ce}^{\perp}$. Assuming that $\mu_{\mathrm{Ce}}=0.55\mu_B$ at 1.8 K and that $\boldsymbol{\mu}_{\mathrm{Ce}}$ is tilted away from the *c* axis by 38° (Ref. 5) and that $q=0.297$, as in $CeRhIn_5$,[2] we calculate an in-plane component of $B_{\mathrm{dip}}^{\perp}=64$ G, which is significantly larger than the measured value at 1.8 K. This situation does not improve when we also take into account the contact hyperfine field $\boldsymbol{B}_c$. Because of the antiferromagnetic arrangement of the $\boldsymbol{\mu}_{\mathrm{Ce}}$ within a CeIn plane and the equal distance of the μ^+ to the four nearest Ce neighbors, we have $\boldsymbol{B}_c=A_0\Sigma_{i=1}^{4}\,\boldsymbol{\mu}_{Ce,i}=0$. More significantly, the magnetic structure as given in Ref. 5 can principally not lead to $B_{\mu}^{\parallel}\neq 0$ at the 1*c* site, neither at the other axially

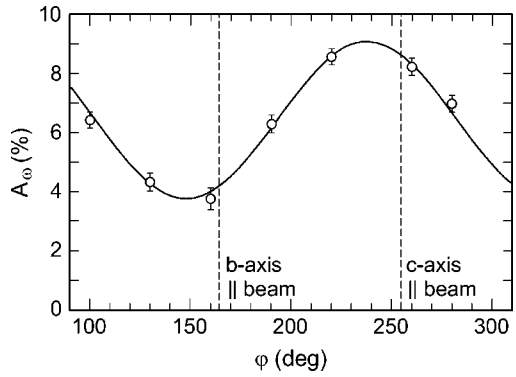

FIG. 6. Orientation dependence of the amplitude A_1 in Eq. (5) in the up positron detector at 1.8 K when rotating the initial polarization $\boldsymbol{P}_{\mu}(t=0)$ in the (b,c) plane. The solid line represents a fit of Eq. (12b) of Ref. 1 to the data yielding azimuthal and polar angles of $\vartheta=90°$ (fixed) and $\varepsilon=-5(2)°$ for the cone axis and a cone aperture of $\Omega=40.2(1.0)°$.

symmetric sites 1*b* and 1*d*. The same problem was encountered in $CeRhIn_5$[1] and it was concluded that there must be a second source for dipole fields, suggested to be the Rh ions. This view appears to be reinforced by the present results and we conclude that also in Ce_2RhIn_8 the Rh ions carry small magnetic moments. To explain the present results we have to postulate that the *c* axis components of the 4 Rh moments, $\boldsymbol{\mu}_{\mathrm{Rh}}^{\parallel}$, next to the *c* site are not completely antiferromagnetically aligned. Two possibilities arise: all four $\mu_{\mathrm{Rh}}^{\parallel}$ are parallel or three are parallel and one is antiparallel. To reproduce the measured $B_{\mu}^{\parallel}=33.7$ G we calculate for the first possibility that $\mu_{Rh}^{\parallel}=0.031\mu_B$, and for second possibility that $\mu_{\mathrm{Rh}}^{\parallel}=0.062\mu_B$, assuming no contact hyperfine field contribution which cannot be ruled out. The presence of a contact hyperfine field would imply larger or smaller values of $\mu_{Rh}^{\parallel}$.

Following Ref. 1 we further assume that the in-plane component $\boldsymbol{\mu}_{\mathrm{Rh}}^{\perp}$ is induced by the nearest Ce neighbors above and below a Rh site, as suggested by the Knight shift results, and that $\mu_{\mathrm{Rh}}^{\perp}$ is oriented midway between the $\boldsymbol{\mu}_{\mathrm{Ce}}^{\perp}$ at those Ce sites. Using the result from the Knight shift measurements, we write, e.g., for the Rh site at (000)

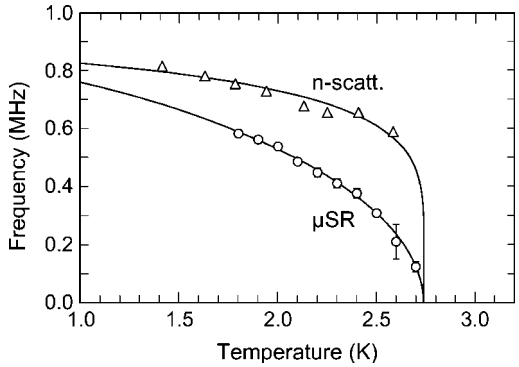

FIG. 7. Temperature dependence of the spontaneous frequency $\nu=\omega/2\pi$. Also shown are the square roots of the neutron magnetic Bragg peak intensities from Ref. 5 normalized to ν at $T=0$ K. The solid lines are fits of Eq. (6) to the data.

$$\boldsymbol{\mu}_{\mathrm{Rh}}^{\perp}(000) = -0.106[\boldsymbol{\mu}_{\mathrm{Ce}}^{\perp}(00z) + \boldsymbol{\mu}_{\mathrm{Ce}}^{\perp}(00-z)],$$

where $z \simeq 0.315$. With this ansatz we calculate $|\boldsymbol{B}_{\mu}| = 36.9$ G, $B_{\mu}^{\perp} = 15$ G for $\boldsymbol{q} = (\frac{1}{2}\frac{1}{2}0.297)$ and $|\boldsymbol{B}_{\mu}| = 44$ G, $B_{\mu}^{\perp} = 28$ G for $\boldsymbol{q} = (\frac{1}{2}\frac{1}{2}0.219)$. The latter values are in excellent agreement with the data; $\delta = 0.219$ implies that $\boldsymbol{\mu}_{\mathrm{Ce}}^{\perp}$ rotates by 78° from the $z \approx 1/3$ plane to the $z \approx 4/3$ plane or by −102° from the $z \approx -1/3$ to the $z \approx 1/3$ plane.

Alternatively we may assume that there is no correlation of $\boldsymbol{\mu}_{\mathrm{Ce}}^{\perp}$ across the Rh planes and hence $\mu_{\mathrm{Rh}}^{\perp}$ may vary from zero to $2 \times 0.106 \mu_{\mathrm{Ce}}^{\perp} \simeq 0.072 \mu_B$. This scenario implies that both the dipole fields from the Ce moments as well as from the induced Rh moments will show a wide distribution. This scenario finds some support in the observation of a relatively large $\Delta B_{\mu}/B_{\mu}$ as quoted earlier. The measured aperture of the precession cone has then to be viewed as an average.

Note that due to the antiferromagnetic arrangement of the $\boldsymbol{\mu}_{\mathrm{Rh}}^{\perp}$ in the (a,b) plane the related net contact hyperfine field at the c site will be zero.

Turning to the 4*i* and 8*r* sites the calculations also predict nonzero field components along the c axis as well as rather strong components in the (a,b) plane. The total field is of the order of 50 G at the 4*i* sites and of 1 kG at the 8*r* sites with the generic position $(\frac{1}{4}\frac{1}{4}\frac{1}{3})$. However, both the c-axis components and the in-(a,b) plane component show alternating signs so that the average over the four 4*i* sites or 8*r* sites around an In atom in the CeIn plane is canceled to zero. This would be in line with the evidence for fast motion of the μ^+ among the 4*i* or 8*r* sites, indicated by the TF data and by the observation that component 2 in ZF below T_N revealed a zero average field. The residual small spread of 0.5 μs^{-1} or ~6 G may reflect the imperfectness of the crystal and/or of the magnetic structure.

As in the case of $CeRhIn_5$ we have no explanation for the origin of $\boldsymbol{\mu}_{\mathrm{Rh}}^{\parallel}$ and its order. It is also not clear why in Ce_2RhIn_8 only a single internal field is observed in contrast to the three spontaneous fields in $CeRhIn_5$.

We note that $B_{\mu}, \Delta B_{\mu}$ and Ω are rather close to the corresponding values of signal 2 in $CeRhIn_5$ ($B_{\mu} = 69$ G, $\Delta B = 23$ G, $\Omega = 37°$). This could suggest that the arrangement of the $\mu_{\mathrm{Rh}}^{\parallel}$ next to the muon site in the present case is the same as in $CeRhIn_5$, namely given by the second possibility considered above. Such an arrangement of the $\mu_{\mathrm{Rh}}^{\parallel}$ in the (a,b) plane is realized, e.g., for the structure proposed in Fig. 8. Of course this structure is totally unrelated to the magnetic structure of the Ce sublattice which may not be unexpected since the $\boldsymbol{\mu}_{\mathrm{Ce}}^{\parallel}$ above and below a Rh site are antiparallel and their combined effect on the intervening Rh is null.

V. SUMMARY

The μSR data show that below T_N the spontaneous internal field has a distinct component along the c axis and randomly oriented components in the (a,b) plane such that the total field is confined to the surface of a cone. The nonzero c-axis component is incompatible with the antiferromagnetic structure of the Ce sublattice as determined by neutron scattering.[5] We also propose that the Rh sublattice carries magnetic moments whose c-axis components may possess an arrangement as shown in Fig. 8 and whose in-plane components assume all possible directions and appear to be induced by the neighboring Ce moments in line with the Knight shift behavior and previous results on $CeRhIn_5$.[5] Concerning the magnetic structure of the Ce lattice it is concluded that the in-plane component of $\boldsymbol{\mu}_{\mathrm{Ce}}$, whose direction is not determined by the neutron scattering experiment, is antiferromagnetically correlated between nearest neighbor CeIn planes and within a plane (as in $CeIn_3$) but the direction of orientation changes arbitrarily or in a correlated fashion between the next nearest CeIn planes. Further, about 2/3 of the implanted μ^+ are located at the c site while the remaining fraction of μ^+ seems to be moving fast between the 4*i* or 8*r* sites around an In atom, possibly forming a tunneling state. Corresponding results were obtained in $CeRhIn_5$.[1]

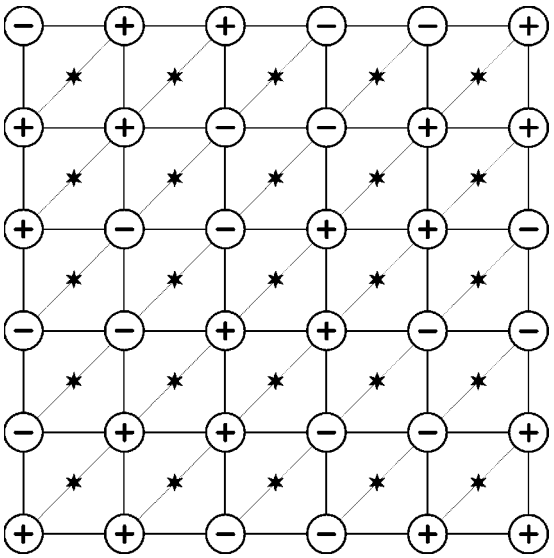

FIG. 8. Possible arrangement of the Rh c-axis magnetic-moment components in the (a,b) plane which leads to three parallel and one antiparallel oriented moments around the μ^+ located at the c site (⋆, at the center of the squares).

ACKNOWLEDGMENTS

We wish to thank the Laboratory for Muon-Spin Spectroscopy ($S\mu S$) and the accelerator crew of the Paul Scherrer Institut (PSI) for providing excellent measuring conditions.

[1] A. Schenck, D. Andreica, F. N. Gygax, D. Aoki, and Y. Ōnuki, Phys. Rev. B **66**, 144404 (2002).
[2] W. Bao, P. G. Pagliuso, J. L. Sarrao, J. D. Thompson, Z. Fisk, J. W. Lynn, and R. W. Erwin, Phys. Rev. B **62**, R14 621 (2000); **63**, 219901(E) (2001); **67**, 099903(E) (2003).
[3] N. J. Curro, P. C. Hammel, P. G. Pagliuso, J. L. Sarrao, J. D. Thompson, and Z. Fisk, Phys. Rev. B **62**, R6100 (2000).
[4] J. D. Thompson *et al.*, see Ref. 11 in Ref. 5.
[5] W. Bao, P. G. Pagliuso, J. L. Sarrao, J. D. Thompson, and Z. Fisk, Phys. Rev. B **64**, 020401(R) (2001).
[6] T. Ueda, H. Shishido, S. Hashimoto, T. Okubo, M. Yamada, Y. Inada, R. Settai, H. Harima, A. Galatanu, E. Yamamoto, N. Nakamura, K. Sugiyama, T. Takeuchi, K. Kindo, T. Namiki, Y. Aoki, H. Sato, and Y. Onuki (unpublished).
[7] See, e.g., A. Schenck, in *Muon Science*, edited by C. L. Lee, S. H. Kilcoyne, and R. Cywinski (IOP, Bristol, 1998).
[8] A. Schenck, F. N. Gygax, D. Andreica, and Y. Ōnuki, J. Phys.: Condens. Matter **15**, 8599 (2003).